Chinese Chemical Letters 34 (2023) 107645

Contents lists available at ScienceDirect

Chinese Chemical Letters

journal homepage: www.elsevier.com/locate/cclet

Efficient blue light-responsed dithienylethenes with exceptional photochromic performance

Ziyong Li[a], Xinyu Gao[a], Haining Zhang[a], Xiaoxie Ma[b], Yifang Liu[a], Hui Guo[a,*], Jun Yin[b,*]

[a] College of Food and Drug, College of Chemistry and Chemical Engineering, Luoyang Key Laboratory of Organic Functional Molecules, Luoyang Normal University, Luoyang 471934, China

[b] College of Chemistry, Key Laboratory of Pesticide and Chemical Biology, Ministry of Education; Hubei International Scientific and Technological Cooperation Base of Pesticide and Green Synthesis; International Joint Research Center for Intelligent Biosensing Technology and Health, Central China Normal University, Wuhan 430079, China

ARTICLE INFO

Article history:
Received 22 March 2022
Revised 25 June 2022
Accepted 27 June 2022
Available online 1 July 2022

Keywords:
Dithienylethene
Photochromism
Fluorescent switching behavior
Visible light
Bifluoroboron β-diketonate (BF_2bdk)
Bacterial imaging

ABSTRACT

Three novel dithienylethenes modified by bifluoroboron β-diketonate fragments have been successfully developed. Upon blue light irradiation, they reached photostationary state within 2–5 s, as well as 100% conversion ratio and photocyclization quantum yield of > 0.70. Such fascinating photochromism were endowed by collaborative role of electron-withdrawing effect of BF_2bdk group to reduce HOMO-LUMO electronic gap for the open isomer, together with intramolecular hydrogen bonds and CH-π interactions favoring antiparallel conformation fixation. Moreover, they displayed specific discrimination and photoswitchable bacterial imaging for *S. aureus*.

In recent years, blooming development of visible light-triggered photoswitches has attracted much attention, as visible light shows low phototoxicity and high penetrability for living organisms [1–3]. As a star photochrome, dithienylethene (DTE) is in possession of excellent photochromic performances, *e.g.*, thermo-stability, robust fatigue resistance and rapid response [4–6]. Over the past few decades, some approaches have been proposed for development of visible-light DTEs, mainly including both direct photoexcitation and indirect photoexcitation *via* energy transfer [1,7,8]. The former is mainly to reduce the HOMO-LUMO energy gap of open form so that the absorption band redshifts to the visible region, which is generally implemented by extending π-conjugation system of DTE [9–11]. However, cumbersome molecular design is required along with deterioration of inherent photochromism in most cases. The indirect excitation generally comprises triplet photosensitizers and upconverting nanoparticles, of which triplet-sensitized photochromism seems to be more appealing for this purpose. For instance, the introduction of a transition metal into DTE has explored based on MLCT mechanism [12]. Undeniably, they often encounter some problems, such as poor cycloreversion quantum yield, metal contamination and high expense [13]. As an alternative, DTE is blended or covalently connected with a proper organic photosensitizer (*e.g.*, biacetyl, 2CzPN) to afford all-visible-light photochromism through a triplet-triplet energy transfer mechanism [14,15]. Whereas relatively low sensitization efficiency and sensitivity to oxygen will hinder their potential applications. Although plenty of strategies and even some new ones have been developed for visible-light DTEs [16,17], the balance between visible-light excitation and photoswitching performance still cannot be achieved. Therefore, searching for a novel approach to fabricate DTE systems with both visible light response and efficient photochromism is highly desirable for further applications.

To strike a balance between structure and performance, some preliminary explorations have been carried out, *e.g.*, the excellent visible-light-photochromism was obtained by introduction of difluoroboron β-diketonate (BF_2bdk) moieties on the central ethene unit [18] or on peripheral thienyl rings (bridged by vinyl bonds) [19,20], respectively, which is mainly due to the fact that electron-withdrawing BF_2bdk group cannot merely extend the conjugated system, but also reduce HOMO-LUMO energy gap. Yet, ideal photochromism for potential applications can still not be afforded. According to previous reports by Morinaka *et al.* [21] and Fukumoto *et al.* [22], specific intramolecular non-covalent interactions were thought to stabilize antiparallel conformation in favor of photocyclization. Hence, we deem that it will provide a possibility for the development of an efficient visible-light-DTE system en-

* Corresponding authors.
E-mail addresses: guohui@lynu.edu.cn (H. Guo), yinj@mail.ccnu.edu.cn (J. Yin).

https://doi.org/10.1016/j.cclet.2022.06.068
1001-8417/

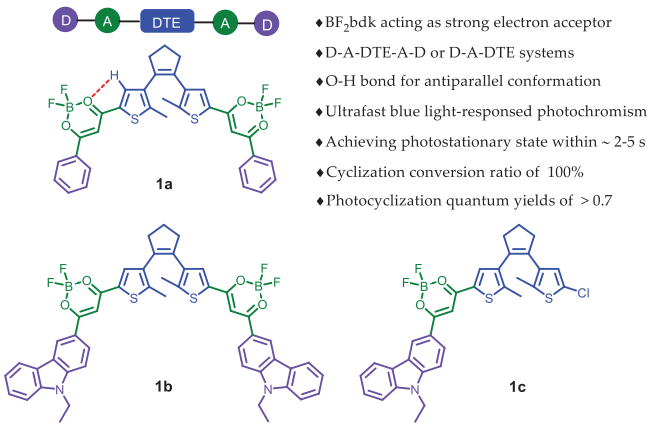

Fig. 1. Chemical structures of blue light-responsed DTEs **1a–1c**.

dowed by the collaborative role of the electron-withdrawing effect of BF_2bdk and intramolecular interactions. Herein, we have presented three novel DTEs directly linked by BF_2bdk fragments on peripheral thienyl pendants (Fig. 1). Upon irradiation with blue light, these DTEs displayed a distinguished photochromic performance. NMR studies and DFT calculations implied the contribution of intramolecular hydrogen bonds and CH-π interactions to antiparallel conformation favoring photocyclization.

The synthetic route of DTEs (**1a–1c**) was depicted in Scheme S1 (Supporting information). The Claisen condensation reaction was carried out between DTE-ester (**5** or **8**) and ketone derivatives (**6** or **7**) in the presence of NaH to afford β-diketone intermediates without any purification, followed by complexation with $BF_3{\cdot}OEt_2$ in yields of 35%–51%. Their structures were fully characterized by ^{1}H NMR, ^{13}C NMR and HRMS (Figs. S1–S9 in Supporting information).

The visible-light photochromic behaviour of **1a–1c** was then investigated in different solvents. As illustrated in Fig. 2a, it was clear that the absorption band of open isomer **1a(o)** centered at 422 nm was observed in toluene, which is derived from intramolecular charge transfer (ICT) transition [23–25]. Upon blue light irradiation at 460–470 nm, a near-infrared absorption band at 742 nm gradually emerged along with the color from yellow to green (Fig. 2a, inset), indicating the formation of closed isomer **1a(c)** (Fig. 2e and Scheme S2 in Supporting information). Amazingly, the photostationary state (PSS) can be achieved after 4 s of irradiation, which should be the fastest response known to date for visible-light DTE systems [1,7]. Moreover, an isosbestic point at 448 nm was observed, clearly indicating the photochromic transformation of **1a(o)** and **1a(c)**. Irradiation with NIR light ($\lambda = 760$–770 nm, 70 s) triggered the cycloreversion reaction to regenerate the initial yellow isomer (Fig. 2b). Further fatigue resistance indicated good reversibility (Fig. 2b, inset), which might be due to blocking of the pathway to photo-byproducts under mild irradiation light [26,27]. As anticipated, a large cyclization quantum yield for **1a** was recorded as 0.77 and its cycloreversion quantum yield was 0.051 in toluene. Similar photochromism was observed in $CHCl_3$ and DMSO when exposed to the same light conditions (Fig. S10 in Supporting information). Compared to that in toluene, the maximum absorption of open and closed isomers showed a distinct bathochromic shift (Fig. 2c and Table S1 in Supporting information), indicating a unique solvent-dependent photochromism. However, it took a longer time to reach PSS, *i.e.*, 5 s in $CHCl_3$ and 9 s in DMSO, implying that the higher the solvent polarity, the

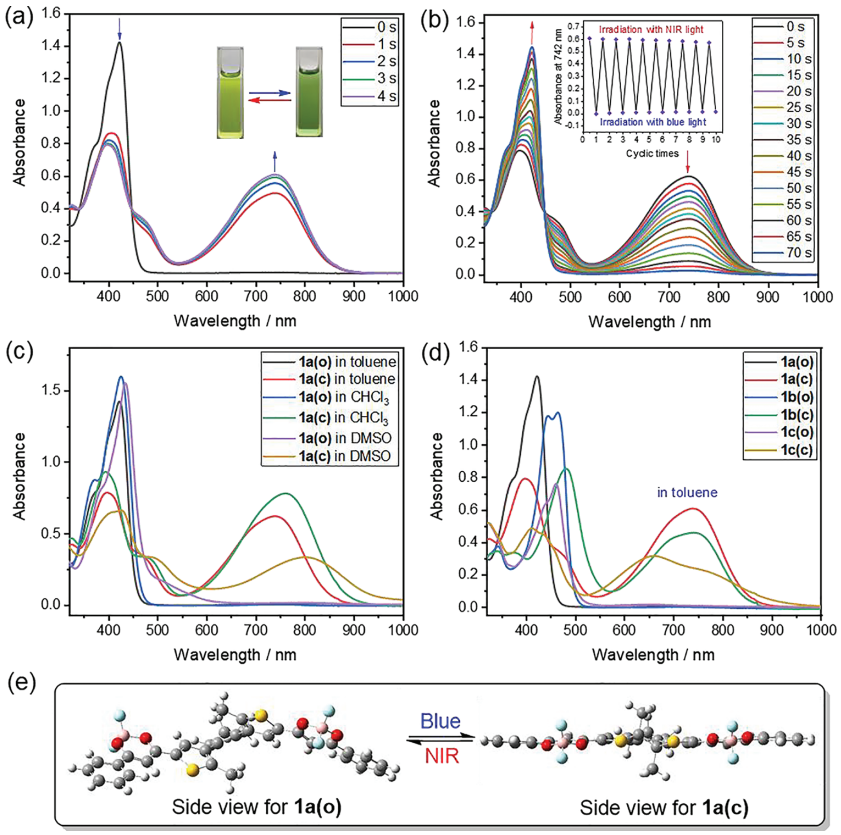

Fig. 2. The UV-vis-NIR absorption spectra changes of **1a** in toluene (2.0×10^{-5} mol/L) upon alternating irradiation with blue light (a) and NIR light (b). Inset: fatigue resistance of **1a**. (c) UV-vis-NIR absorption spectra of **1a(o)** and **1a(c)** in various solvents. (d) UV-vis-NIR absorption spectra of **1a–1c**. (e) Optimized geometric structures of **1a(o)** and **1a(c)**.

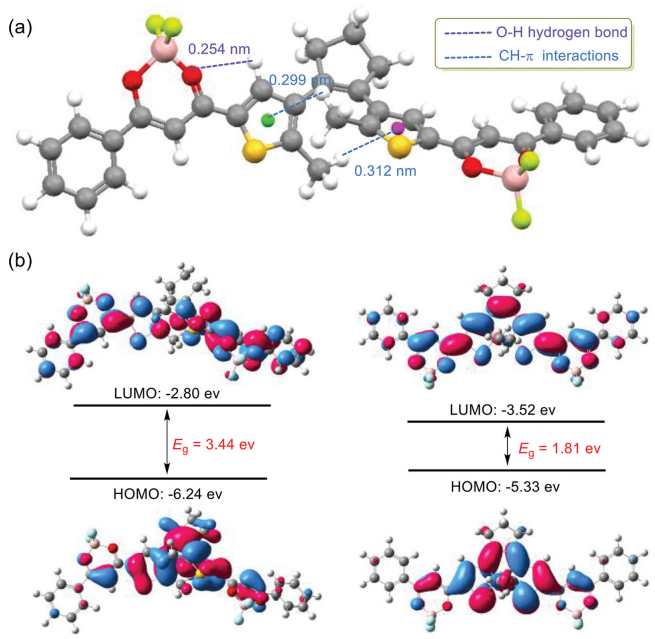

Fig. 3. (a) Side view of optimized geometry of ring-open isomer **1a(o)**, in which the dotted lines indicate O–H hydrogen bonds and CH-π interactions between methyl groups at reactive carbons and thienyl rings; (b) frontier molecular orbital profiles of ring-open and -closed isomers of **1a** based on DFT calculations (*in vacuo*) *via* the Gaussian 09 program (B3LYP/6-31G* level).

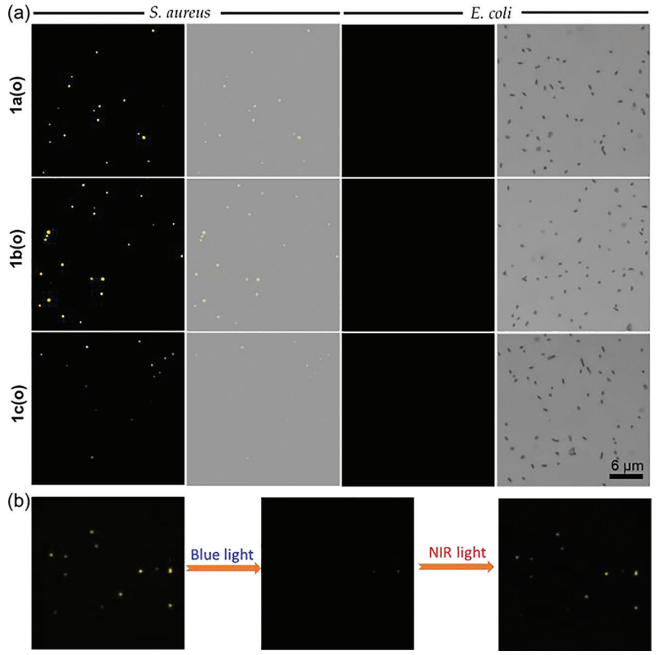

Fig. 4. (a) Fluorescence and merged images of bacteria (*S. aureus* and *E. coli*) incubated with **1a(o)**, **1b(o)** and **1c(o)**. (b) Photoswitchable bacterial imaging of **1a(o)** toward *S. aureus* upon alternating irradiation.

slower the cyclization. As expected, the corresponding cyclization quantum yields decreased as the solvent polarity increased (Table S1). In brief, **1a** presented an exceptional blue light-triggered photochromism in different solvents.

Subsequently, the photoisomerization of **1a** was further analyzed *via* ^{1}H NMR spectral variations in DMSO-d_6. Compared with **1a(o)**, all the protons in **1a(c)** showed a significant upfield shift due to electron shielding effect of closed form with an extended π-conjugation (Fig. S11 in Supporting information). To our excitement, the photocyclization conversion ratio at PSS was determined to be 100% according to ^{1}H NMR results. Surprisingly, the signals of methyl protons (H_c) and thienyl proton (H_d) in **1a(o)** appeared at δ 2.05 and δ 8.64, respectively, which separately showed a slight upfield shift and a significant downfield shift compared with our previously reported BF_2bdk-DTE analogues (*e.g.*, for CDB1 in Fig. S14 in Supporting information, the corresponding proton signals appeared at δ 2.15 (methyl-H_c) and δ 7.22 (thienyl-H_d)) [19]. So it would be unreasonable to evaluate the effect of BF_2bdk group on hydrogen protons in DTE unit by only considering its stronger electron-withdrawing ability than BF_2bdk-DTE analogues like CDB1. If so, the H_c signal in **1a(o)** should also appear at a lower field than 2.15 ppm, rather than 2.05 ppm. According to previous reports [21,22], the upfield shift of methyl protons originated from intramolecular CH-π interactions between the methyl group and the other side-plane. Besides, such a significant downfield shift for H_d ($\Delta\delta = 1.42$ ppm) might be synergistic role of electron-withdrawing effect of BF_2bdk and intramolecular C–H···O weak hydrogen bond between O in BF_2bdk and H in thienyl group. Therefore, these results indicated the presence of intramolecular C–H···O weak hydrogen bond and CH-π interactions between the methyl group and the conjugated plane of thiophene-BF_2bdk-benzene on the other side, which would favor fixation of the antiparallel conformation.

To further confirm intramolecular interactions for **1a**, DFT calculations were performed [28]. As shown in Fig. 3a, **1a** presented an antiparallel conformation. Particularly, the distance between H in thienyl and O in BF_2bdk was estimated to be 0.254 nm, which is shorter than the sum of the van der Waals radii of the H (0.120 nm) and O atom (0.152 nm), clearly implying intramolecular hydrogen bonding. Moreover, intramolecular CH-π interactions were also proposed by shorter distances between H atoms on methyl and the opposite plane of thiophene-BF_2bdk-benzene triad (0.299 and 0.312 nm). Therefore, DFT calculations further verified the role of intramolecular hydrogen bond and CH-π interactions in fixing antiparallel conformation. In addition, HOMO electron densities of **1a(o)** was primarily distributed in central DTE unit, and the LUMO was localized over the BF_2bdk fragments resulting from electron-deficient effect of BF_2 (Fig. 3b), indicating A-DTE-A type architecture. For **1a(c)**, the HOMO was roughly distributed over the whole molecular skeleton and the LUMO was localized in the central DTE unit. Expectedly, **1a(c)** presented a smaller energy gap ($\Delta E_g = 1.81$ eV) than **1a(o)** ($\Delta E_g = 3.44$ eV) due to its extended π-conjugation.

Whereafter, photochromism of carbazole-substituted analogues **1b** and **1c** were further evaluated. As shown in Fig. 2d, Figs. S12, S13 and Scheme S2 (Supporting information), excellent photochromism for **1b** and **1c** was also found under the same irradiation conditions. By contrast, a striking bathochromic-shift ($\Delta\lambda = 39$–49 nm) for open isomers **1b(o)** and **1c(o)** was observed due to the electron-donating carbazole group. For closed isomers, bilateral **1b(c)** showed a negligible red-shift while an obvious blue shift was detected for unilateral **1c(o)**. Beyond that, introduction of electron-donating carbazole groups in **1b** and **1c** accelerated the two-way reaction rate of both cyclization and cycloreversion under the same conditions compared with benzene-modified **1a**. Moreover, **1c** presented higher photochromic quantum yields than those of **1a** and **1b** in DMSO (Table S1). High photocyclization conversion ratios were also recorded as 100% for **1b** and 88% for **1c**, respectively (Figs. S15, S16 and Table S2 in Supporting information). Similar DFT calculation results of **1b** and **1c** were obtained for optimized structures, intramolecular interactions and electron distributions (Figs. S17–S19 in Supporting information). These results in-

dicated that electron-donating group attached to BF_2bdk was favorable for further improving visible-light photochromism in this system.

Given the excellent luminescence of BF_2bdk complexes, the following exploration focused on the fluorescence-switching of **1a–1c**. As depicted in Fig. S20a and Table S3 (Supporting information), **1a(o)** exhibited a bright green fluorescence at 493 nm prior to irradiation in toluene, whose relative photoluminescence quantum yield was estimated to be $\phi_f = 0.21$. Upon blue light irradiation, the emission peak was gradually decreased along with green fluorescence fading, probably owing to efficient energy transfer between the excited BF_2bdk and closed DTE moieties [29–31]. After reaching PSS in 4 s, the fluorescence intensity of **1a(o)** was quenched by *ca*. 90%, which returned to the original intensity after irradiation with NIR light. Besides, such switching process could reversibly conducted ten cycles with negligible degradation (Fig. S20b in Supporting information). By contrast, the emission peak of **1a(o)** displayed a significant red-shift in $CHCl_3$ (524 nm, yellow-green) and DMSO (544 nm, orange) (Fig. S20c in Supporting information). And similar fluorescent switching behavior was observed in $CHCl_3$ and DMSO (Fig. S21 in Supporting information). Moreover, **1b** and **1c** presented the red-shifted fluorescence-switching process under the same conditions (Figs. S20d, S22, S23 and Table S3 in Supporting information).

Inspired by their excellent fluorescence-switching behavior, we selected Gram-positive *S. aureus* and Gram-negative *E. coli* for the preliminary assessment of the bacteria staining performance of **1a–1c**. After incubated with fluorescent dyes **1a–1c**, the distinct fluorescence signal was visualized in *S. aureus*, while almost no fluorescence signal was detected for *E. coli* (Fig. 4a), indicating specific discrimination for *S. aureus* and *E. coli*, which is due to multilayer outer membrane structures of Gram-negative bacteria [32,33]. Besides, photoswitchable bacterial imaging of **1a(o)** toward *S. aureus* was conducted upon alternating irradiation with blue and NIR light (Fig. 4b). When *S. aureus* stained with **1a(o)** was exposed to blue light for 80 s, the distinct fluorescence signals were gradually vanished, indicating **1a(o)** was transformed to **1a(c)** in *S. aureus*. Upon irradiation with NIR light, the fluorescence signals came back. It was noted that there was no significant decrease in the number of *S. aureus* after repeating the above operation several times. It is worth noting that photoswitching behavior in bacteria is consistent with that in solutions.

In summary, three novel BF_2bdk-functionalized DTEs were successfully developed. Upon blue light irradiation, they can reach PSS in *ca.* 2–5 s, as well as 100% conversion ratio and up to >0.70 of $\varphi_{o\text{-}c}$. Such exceptional visible light-photochromism were endowed by the collaborative role of the electron-withdrawing effect of BF_2bdk, together with intramolecular C–H···O hydrogen bond and CH-π interactions favoring fixation of photoreactive antiparallel conformation. Moreover, they displayed specific discrimination and photoswitchable imaging for *S. aureus*. This successful example can provide guidance for further development of more efficient visible-light-DTE systems for biomedical applications.

Declaration of competing interest

There are no conflicts to declare.

Acknowledgments

The authors acknowledge financial support from the Natural Science Foundation of Henan Province (No. 222300420501), the Science and Technology Project of Henan Province (No. 212102210549), and the Key Scientific Research Project of Higher Education of Henan Province (No. 22A430007), and National College Students Innovation and Entrepreneurship Training Program (No. 202110482010).

Supplementary materials

Supplementary material associated with this article can be found, in the online version, at doi:10.1016/j.cclet.2022.06.068.

References

[1] D. Bléger, S. Hecht, Angew. Chem. Int. Ed. 54 (2015) 11338–11349.
[2] M. Wegener, M.J. Hansen, A.J.M. Driessen, W. Szymanski, B.L. Feringa, J. Am. Chem. Soc. 139 (2017) 17979–17986.
[3] H. Chen, W. Chen, Y. Lin, et al., Chin. Chem. Lett. 32 (2021) 2359–2368.
[4] H. Tian, S. Yang, Chem. Soc. Rev. 33 (2004) 85–97.
[5] M. Irie, T. Fukaminato, K. Matsuda, S. Kobatake, Chem. Rev. 114 (2014) 12174–12277.
[6] A.S. Lubbe, W. Szymanski, B.L. Feringa, Chem. Soc. Rev. 46 (2017) 1052–1079.
[7] H. Wang, H.K. Bisoyi, X. Zhang, F. Hassan, Q. Li, Chem. Eur. J. 28 (2022) e202103906.
[8] Z. Li, C. He, Z. Lu, P. Li, Y.P. Zhu, Dyes Pigments 182 (2020) 108623.
[9] T. Fukaminato, T. Hirose, T. Doi, et al., J. Am. Chem. Soc. 136 (2014) 17145–17154.
[10] T. Sumi, T. Kaburagi, M. Morimoto, et al., Org. Lett. 17 (2015) 4802–4805.
[11] N.M.W. Wu, M. Ng, W.H. Lam, H.L. Wong, V.W.W. Yam, J. Am. Chem. Soc. 139 (2017) 15142–15150.
[12] C.C. Ko, V.W.W. Yam, Acc. Chem. Res. 51 (2018) 149–159.
[13] J. Lu, B. Pattengale, Q. Liu, et al., J. Am. Chem. Soc. 140 (2018) 13719–13725.
[14] S. Fredrich, R. Gostl, M. Herder, L. Grubert, S. Hecht, Angew. Chem. Int. Ed. 55 (2016) 1208–1212.
[15] Z. Zhang, W. Wang, P. Jin, et al., Nat. Commun. 10 (2019) 4232.
[16] J. Xu, H. Volfova, R.J. Mulder, et al., J. Am. Chem. Soc. 140 (2018) 10482–10487.
[17] H. Xi, Z. Zhang, W. Zhang, et al., J. Am. Chem. Soc. 141 (2019) 18467–18474.
[18] C.T. Poon, W.H. Lam, H.L. Wong, V.W.W. Yam, J. Am. Chem. Soc. 132 (2010) 13992–13993.
[19] Z. Li, Y. Pei, Y. Wang, et al., J. Org. Chem. 84 (2019) 13364–13373.
[20] Z. Li, Y. Dai, Z. Lu, et al., Chem. Commun. 55 (2019) 13430–13433.
[21] K. Morinaka, T. Ubukata, Y. Yokoyama, Org. Lett. 11 (2009) 3890–3893.
[22] S. Fukumoto, T. Nakashima, T. Kawai, Angew. Chem. 123 (2011) 1603–1606.
[23] X. Wu, D. Li, J. Li, et al., Chin. Chem. Lett. 32 (2021) 1937–1941.
[24] X. Ma, W. Chi, X. Han, et al., Chin. Chem. Lett. 32 (2021) 1790–1794.
[25] D. Shi, S. Chen, B. Dong, et al., Chem. Sci. 10 (2019) 3715–3722.
[26] M. Herder, B.M. Schmidt, L. Grubert, et al., J. Am. Chem. Soc. 137 (2015) 2738–2747.
[27] X. Li, D. Shi, Y. Song, et al., Chin. Chem. Lett. 33 (2022) 1572–1576.
[28] M.J. Frisch, G.W. Trucks, H.B. Schlegel, et al.Gaussian 09, Revision B.01, Gaussian, Inc., Wallingford CT, 2010.
[29] T. Kawai, T. Sasaki, M. Irie, Chem. Commun. (2001) 711–712.
[30] D. Li, W. Chen, S.H. Liu, X. Chen, J. Yin, Chin. Chem. Lett. 31 (2020) 2891–2896.
[31] Y. Gao, Y. Hu, Q. Liu, et al., Angew. Chem. Int. Ed. 60 (2021) 10756–10765.
[32] G. Li, J. Wang, D. Li, et al., Chin. Chem. Lett. 32 (2021) 1527–1531.
[33] M. Kang, C. Zhou, S. Wu, et al., J. Am. Chem. Soc. 141 (2019) 16781–16789.